# Sox18 and Sox7 play redundant roles in vascular development

Solei Cermenati,[1] Silvia Moleri,[1] Simona Cimbro,[2] Paola Corti,[1] Luca Del Giacco,[2] Roberta Amodeo,[1] Elisabetta Dejana,[1,3] Peter Koopman,[4] Franco Cotelli,[2] and Monica Beltrame[1]

[1]Dipartimento di Scienze Biomolecolari e Biotecnologie, Università degli Studi di Milano, Milan, Italy; [2]Dipartimento di Biologia, Università degli Studi di Milano, Milan, Italy; [3]FIRC Institute of Molecular Oncology (IFOM), Milan, Italy; and [4]Institute for Molecular Bioscience, The University of Queensland, Brisbane, Australia

**Mutations in *SOX18* cause the human hypotrichosis-lymphedema-telangiectasia (HLT) syndrome. Their murine counterparts are the spontaneous *ragged* mutants, showing combined defects in hair follicle, blood vessel, and lymphatic vessel development. Mice null for *Sox18* display only mild coat defects, suggesting a dominant-negative effect of *Sox18/ragged* mutations and functional redundancy between Sox18 and other Sox-F proteins. We addressed this point in zebrafish. The zebrafish homologs of *Sox18* and of *Sox7* are expressed in angioblasts and in the endothelial component of nascent blood vessels in embryos. Knockdown of either gene, using moderate doses of specific morpholinos, had minimal effects on vessels. In contrast, simultaneous knockdown of both genes resulted in multiple fusions between the major axial vessels. With combined use of transgenic lines and molecular markers, we could show that endothelial cells are specified, but fail to acquire a correct arteriovenous identity. Venous endothelial cell differentiation was more severely affected than arterial. Thus, *sox7* and *sox18* play redundant but collectively essential roles in the establishment of proper arteriovenous identity in zebrafish. Our data suggest that a defect in arteriovenous identity could be responsible for the formation of telangiectases in patients with HLT. (Blood. 2008;111:2657-2666)**



## Introduction

The acquisition of arterial and venous identity is an early event in endothelial cell differentiation, preceding the onset of blood circulation. Pioneering work in the zebrafish has revealed that the acquisition of arterial identity is governed by a genetic network including Shh, VEGF, and Notch signaling.[1-3] Many aspects of this regulatory cascade are also conserved in mammals.[4] More recently, the acquisition of venous identity was shown not to occur by default but rather to be genetically controlled. The orphan nuclear receptor COUP-TFII induces venous endothelial cell differentiation by suppressing Notch signaling.[5] Although chick-quail grafting experiments point to an initial plasticity (ie, nascent endothelial cells are able to change their arteriovenous identity depending on the surrounding context), it is becoming clear that arterial and venous angioblasts segregate from the beginning of vasculogenesis.[6] The ephrin/Eph system is involved in the establishment of arteriovenous (AV) cell identity, and is important for the segregation between arteries and veins. The transmembrane ligand ephrinB2, and its cognate tyrosine kinase receptor EphB4, are exclusively expressed by arterial and venous endothelial cells, respectively, both in mouse and in zebrafish, and this molecular distinction is essential to establish a functional hierarchical vascular network.[6]

Arteriovenous malformations (AVMs) are frequently induced by a loss of arterial or venous cell identity.[7] In humans, hereditary hemorrhagic telangiectasia (HHT) is a vascular dysplasia characterized by anomalous fusion of arterioles and venules, leading to telangiectases in the skin and mucocutaneous tissues and intrahepatic and pulmonary AVMs. HHT type 1 and type 2 are both caused by autosomal dominant mutations in the transforming growth factor beta (TGF-β) receptors ENG and ALK1, respectively. *Alk1*$^{-/-}$ homozygous mouse embryos exhibit large AV shunts between major arteries and veins, linked to a loss of ephrinB2 expression in the vasculature.[8]

Hypotrichosis-lymphedema-telangiectasia (HLT) is a human syndrome characterized by the association of the 3 pathologic traits.[9] Dominant and recessive forms of this syndrome are linked to mutations in the *SOX18* gene. SOX (SRY-related HMG-box) proteins are a family of transcription factors characterized by an HMG-box DNA binding domain; they are present throughout the animal kingdom and play key roles in embryonic development.[10,11] Twenty SOX genes are present in mammals, subdivided in several groups on the basis of the similarities among HMG-boxes.[12] *SOX18* belongs to SOX subgroup F, together with the closely related *SOX7* and *SOX17*. The spontaneous *ragged* mutant mice, first described in the 1950s,[13,14] represent the murine counterpart of the HLT syndrome and are characterized by defects in vascular, hair follicle, and lymphatic development. Closely spaced mutations within the mouse *Sox18* gene underlie the 4 allelic variants of the *ragged* phenotype.[15,16] These mutations alter the transactivation and C-terminal domains of the Sox18 protein, without affecting its DNA binding domain, and they act genetically in a semidominant fashion. The most severe allele, *ragged-opossum* (*RaOp*), causes embryonic lethality before embryonic day (E) 11.0 in homozygous mutant mice.[15,17] On the other hand, *Sox18*-null mice are viable and present only a mild coat defect.[18] It has been suggested that related SOX proteins can compensate for the absence of SOX18 in null

Submitted July 13, 2007; accepted December 12, 2007. Prepublished online as *Blood* First Edition paper, December 19, 2007; DOI 10.1182/blood-2007-07-100412.

S. Cermenati and S.M. equally contributed to this paper.

The online version of this article contains a data supplement.

The publication costs of this article were defrayed in part by page charge payment. Therefore, and solely to indicate this fact, this article is hereby marked "advertisement" in accordance with 18 USC section 1734.

mice, while the mutations in *ragged* mice give rise to truncated SOX18 proteins that act in a dominant-negative fashion and interfere with functionally redundant SOX transcription factors.[18,19] *Sox7* and *Sox17* have been found to be expressed together with *Sox18* during vascular development in mouse,[20] and may provide the suggested redundancy.

We decided to specifically address the functional redundancy of Sox-F genes in vascular development by making use of the zebrafish model system. We first identified the zebrafish *sox18* and *sox7* genes and showed that they have largely overlapping expression in the developing vasculature. Simultaneous partial knockdown of both genes, but not of either one, using moderate amounts of specific morpholinos, caused a block of trunk/tail blood circulation. The expression of several endothelial markers was altered in the double morphants from the very first stages of vasculogenesis. Venous endothelial markers were more affected than arterial ones. The double morphants presented several shunts between the dorsal aorta and the cardinal vein.

Our data indicate that *sox18* and *sox7* are functionally redundant, but collectively essential in the differentiation of vascular endothelial cells and in their acquisition of a full AV identity.

## Methods

### Zebrafish lines and maintenance

Zebrafish were raised and maintained according to established techniques.[21] The following strains were used: AB (obtained from the Wilson lab, University College London, London, United Kingdom), tg(*fli1*:EGFP)$^{y1}$ (Ref. 22) (from the Lawson lab, University of Massachusetts Medical School, Boston), tg(*flk1*:EGFP) (Ref. 23) (from the Stainier lab, University of California at San Francisco), and tg(*gata1*:dsRed) (Ref. 24) (from the Zon lab, Children's Hospital, Boston, MA). Fixed *clo*$^{s5}$ embryos were kindly provided by M. Gering (Nottingham, United Kingdom).

### Morpholinos

Antisense morpholinos (MOs; Gene Tools, Philomath, OR) were designed against the AUG translation start site region and the 5′ untranslated region (UTR): *sox7*-MO1, 5′-ACGCACTTATCAGAGCCGCCATGTG-3′; *sox18*-MO1, 5′-TATTCATTCCAGCAAGACCAACACG-3′; *sox7*-MO4, 5′-CTCAAACTTTGTTTCTCGGGCGCAG-3′; and *sox18*-MO4, 5′-CCAGCAAGACCAACACGATTAAAGC-3′. Splice MOs targeting the 5′ splice site of the intron within the HMG-box coding region were designed as follows: *sox7*-MO2, 5′-GTTAAAATCTTACCAAGCATCTTGC-3′; and *sox18*-MO2, 5′- GTGAGTGTCTTACCCAGCATTTTAC-3′. MOs, diluted in Danieau buffer,[25] were injected at 1- to 2-cell stage. Escalating doses of each MO were tested for phenotypic effects; as control for unspecific effects, each experiment was performed in parallel with a std-MO (standard control oligo) with no target in zebrafish embryos. For double knockdown experiments, we usually injected 250 fmol/embryo of each MO1, 750 fmol/embryo of each MO2, and 500 fmol/embryo of each MO4. *scl* spliceMO,[26] kindly provided by the Patient lab (Oxford, United Kingdom), was injected at 1 pmol/embryo.

### RT-PCR

RNA samples were extracted with TOTALLY RNA isolation kit (Ambion, Austin, TX), treated with RQ1 RNase-Free DNase (Promega, Madison, WI), and retrotranscribed with random hexamers (High Capacity cDNA Archive kit; Applied Biosystems, Foster City, CA), according to the manufacturers' instructions. Real-time polymerase chain reaction (PCR) was performed using the TaqMan methodology (Applied Biosystems) and an ABI thermocycler (Applied Biosystems); details on primers and probes are available on request. Additional details can be found in the legend for Figure S1 (available on the *Blood* website; see the Supplemental Materials link at the top of the online article).

### In situ hybridization and imaging

Whole-mount in situ hybridizations (ISHs) were carried out essentially as described.[26,27] For double ISHs, fluorescein probes were purified on Spin Post-Reaction Clean-Up Columns (Sigma-Aldrich, St Louis, MO) prior to use, and red staining was obtained with an INT Red (Sigma-Aldrich)/BCIP (Roche, Mannheim, Germany) mix. The following probes were synthesized as described in corresponding papers: *flk1*,[28] *fli1*,[29] *lmo2* and *flt4*,[30] *gata1* and *gata2*,[31] *notch3*,[1] *deltaC*,[32] *scl*,[33] *vegf165*,[34] *dab2*,[35] *etsrp* and *admr*,[36] *ang1*,[37] *radar*,[38] *cdh5*,[39] *vsg1*,[40] *grl*,[2] and *kdrb*.[41] *flt1* was kindly provided by S. Schulte-Merker (Ultrecht, The Netherlands); *efnB2a* and *ephB4* were kindly provided by R. Patient.

For the *sox18* probe, a *Bgl*II-*Kpn*I fragment from IMAGE clone 6790334 was subcloned into pBSKS$^+$; the resulting plasmid was digested with *Sma*I and transcribed with T7 RNA Polymerase (Roche). For the *sox7* probe, the IMAGE clone 7044541 was digested with *Bam*HI and transcribed with T7 RNA Polymerase (Roche).

Images were taken with a Leica MZFLIII epifluorescence stereomicroscope equipped with a DFC 480 R2 digital camera and IM50 Leica imaging software (Leica, Wetzlar, Germany). Confocal microscopy was performed on a Leica TCS SP2 AOBS microscope, equipped with an argon laser. Images were processed using the Adobe Photoshop software (Adobe, San Jose, CA). Movies were processed using the QuickTime Player software (Apple, Cupertino, CA).

### Alkaline phosphatase staining and chemical treatments

Alkaline phosphatase staining was performed as described.[42]

2,3-butanedione monoxime (2,3-BDM; Sigma) was added at 8 mM to 24-hpf (hours postfertilization) dechorionated embryos to block heartbeat, as previously described.[43]

### Cryosections and plastic sections

Tg(*fli1*:EGFP)$^{y1}$ embryos at 30 hpf were fixed at room temperature in 4% paraformaldehyde/phosphate-buffered saline (PBS). Cryosections (24 μm) were obtained as described[42] and analyzed by confocal microscopy.

Embryos for histologic analysis were fixed at room temperature in 1.5% glutaraldehyde/4% paraformaldehyde/cacodylate buffer (pH7.2), postfixed in 1% osmium tetroxide, embedded in an Epon-Araldite mixture, and sectioned with an ultramicrotome. Semithin plastic sections (1-1.5 μm) were stained with violet gentian and basic fuchsin. Images were taken with an Olympus BH2 microscope (Tokyo, Japan), equipped with a Leica DFC320 digital camera.

## Results

### *Sox18* and *Sox7* homologs in zebrafish

By using the mouse sequences as queries in combined searches of genomic and expressed sequence tag (EST) databases (Ensembl, National Center for Biotechnology Information [NCBI]), we identified cDNA clones corresponding to putative *Sox7* and *Sox18* orthologs in zebrafish. These clones were obtained from the I.M.A.G.E. consortium (Lawrence Livermore National Laboratory, Livermore, CA) through MRC geneservice (Cambridge, United Kingdom). The complete sequences (Sox7, 390 aa; Sox18, 431 aa) were highly related to previously identified homologs in mammals, chick, *Xenopus*, and *Fugu rubripes* (Figure S1). Both proteins contain the β-catenin binding motif[44] that is present in all Sox-F group proteins with the notable exception of zebrafish Sox17. Zebrafish Sox7, Sox17, and Sox18 share very high amino acid identity within the HMG-box domain (> 85% in pairwise comparisons), but are less related to each other than to their mammalian homologs.

About 20% of the zebrafish genome is duplicated due to an event before the teleost radiation,[45] but we failed to find duplicates

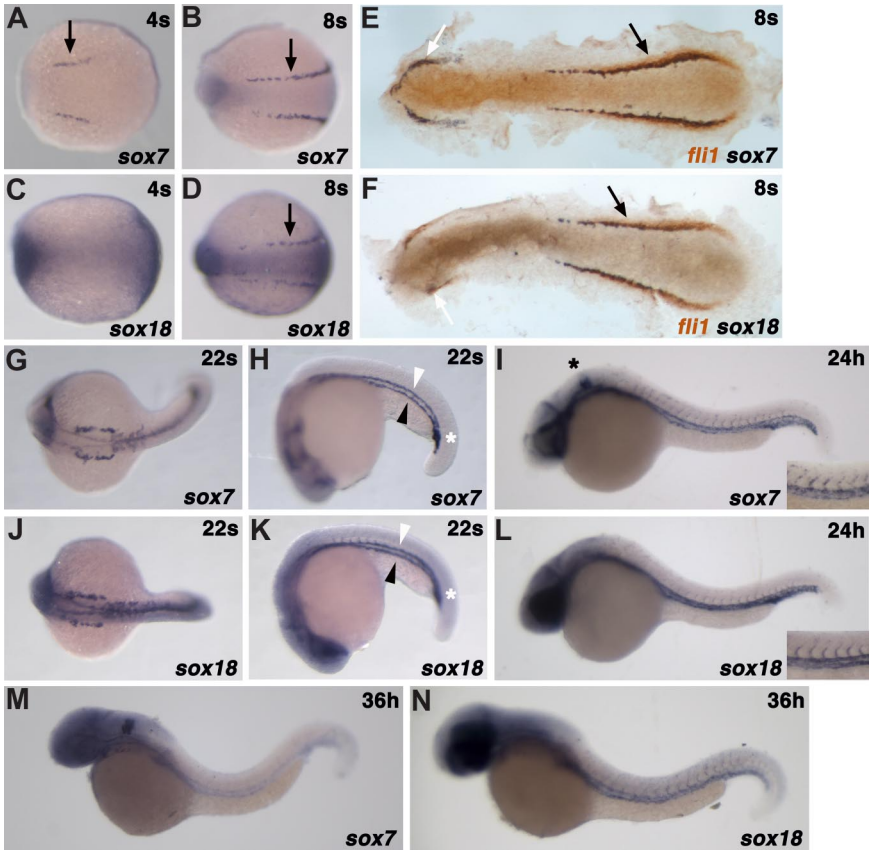


**Figure 1. *sox18* and *sox7* are coexpressed in endothelial cells and their precursors.** The expression of the 2 genes was analyzed by ISH at various developmental stages, alongside with known markers. The expression of the 2 genes in endothelial cells and their precursors appears to be largely overlapping, although *sox7* starts being detectable, and fades away, slightly earlier than *sox18*. (A,C) 4 somites, 40× magnification; (B,D-F) 8 somites; white and black arrows point to the ALM and PLM, respectively. (G,H,J,K) 22 somites; the developing DA, PCV, and ICM are marked with white arrowheads, black arrowheads, and white asterisks, respectively. (I,L) 24 hpf; higher magnifications inserts on the right show expression in the DA, PCV, and ISVs. A black asterisk in panel I marks *sox7* expression in the otic vesicles. (M,N) 36 hpf. In all images, embryos are shown anterior to the left. In flat-mount images (E,F), double ISHs are presented to show colocalization of *sox7* and *sox18* with the innermost *fli1*-positive cells in the PLM. (A-D,G,J) Dorsal views. (H-N) Lateral views.

for *sox7* and *sox18*, which map on chromosomes 20 and 23, respectively (Zv6 assembly; http://www.sanger.ac.uk/Projects/D_rerio). Both genes have a single intron within the sequence coding for the HMG-box, in a conserved position relative to their mammalian orthologs.[11]

We analyzed the expression of the 3 zebrafish Sox-F group genes during embryonic and early larval development by real-time reverse transcription (RT)–PCR (Figure S2). As expected from its role in endoderm development,[46] the *sox17* gene is expressed at maximum levels during gastrulation while its expression drops during somitogenesis. In contrast, *sox7* and *sox18* expression levels are low during gastrulation; they start increasing in somitogenesis and peak at around 1.5 dpf (days postfertilization). At this stage, blood circulation has already started, and the vascular tree is actively being remodeled.

*Sox18* is expressed transiently in the endothelial component of the developing blood vessels in mouse and chicken (reviewed by Downes and Koopman[19]). Mouse *Sox7* and *Sox18* expressions are parallel in diverse locations, including the developing embryonic vasculature.[20,47] *Sox7* expression in the embryonic vasculature was recently reported also in *Xenopus laevis*.[48]

Our whole-mount ISH analysis (Figure 1) reveals that during somitogenesis zebrafish *sox7* and *sox18* are both expressed in bilateral stripes corresponding to the posterior lateral plate mesoderm (PLM) and, at a lower level, in the anterior lateral plate mesoderm (ALM). ALM and PLM are the regions where hemangioblasts, the presumptive common precursors of blood and endothelial cells, are thought to reside.[29,33] *sox7* transcripts are detectable at 4-somite stage, and *sox18* at 6- to 8-somite stage (Figure 1A-D). *sox7* and *sox18* are expressed in the innermost PLM *fli1*-positive cells, corresponding to endothelial cell precursors,[29,49] as revealed by double ISH (Figure 1E,F). The *sox7* expression domain in the PLM appears slightly broader than that of *sox18* (Figure 1E,F; data not shown).

During vasculogenesis in zebrafish, 2 waves of angioblast migration from lateral plate mesoderm to the midline give rise to 2 axial vascular cords (the arterial one preceding the venous) that subsequently lumenize. Secondary vessel formation by angiogenesis follows after the coalescence of arterial and venous angioblasts at the midline. We could see *sox7* and *sox18* expressing cells migrating from the PLM to the midline (data not shown). Both *sox7* and *sox18* marked the developing axial and intersomitic vessels (ISVs), and the intermediate cell mass (ICM), where endothelial and blood cell precursors reside. *sox7* and *sox18* were also expressed in the developing head vasculature.

*sox7* and *sox18* are differentially expressed in other regions of the embryo: *sox7* staining was clearly associated with the developing otic vesicles (Figure 1I), whereas more diffuse *sox18* staining was visible in the rostral region of the embryo from early somitogenesis (Figure 1C,D,F). At around 24 hpf, *sox18* was expressed in rostral parts of the central nervous system, notably in the eye region (Figure 1L).

### Expression of *sox7* and *sox18* in *cloche* mutants and *scl*-morphants

Based on their expression domains, it seemed likely that *sox7* and *sox18* could play a role in zebrafish vascular development. To place both genes in the hierarchy of genes controlling endothelial cell differentiation and blood vessel formation, we examined their expression in the *cloche* mutant (*clo*) and in wild-type embryos injected with a morpholino directed against *scl* ($scl^{mo}$). The zebrafish *clo* mutation affects a very early step in differentiation of blood and endothelial cells,[50] at the level of the putative hemangioblast. The *scl* gene acts downstream of *clo*[51]

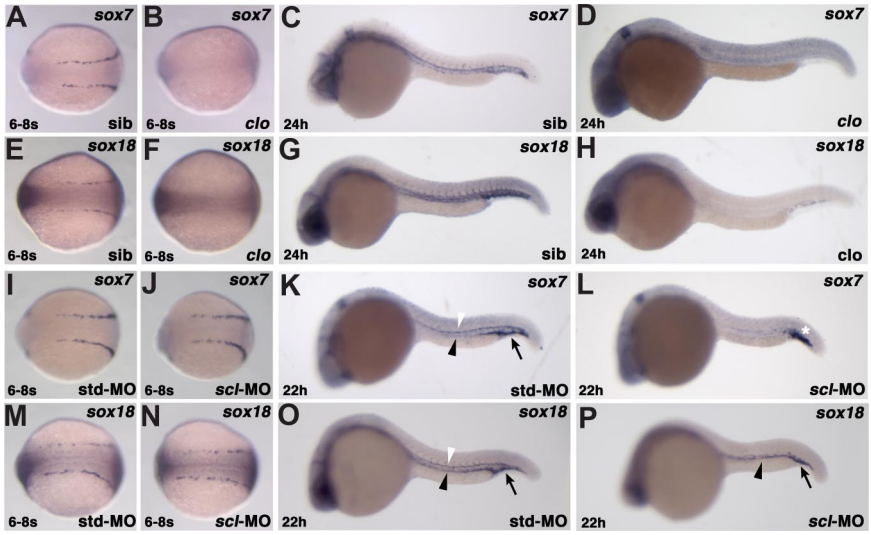


**Figure 2. The early endothelial expression of *sox18* and *sox7* is affected in *cloche* mutants but not in *scl*-morphants.** The expression of *sox7* and *sox18* was analyzed by ISH in pools of embryos from *cloche*$^{s5}$ heterozygotes clutches at 6 to 8 somites (A,B,E,F) and 24 hpf (C,D,G,H). Control hybridizations carried out with *gata1* or *cdh5* probes, at the 2 developmental stages, confirmed that *cloche* mutant embryos were present at the expected Mendelian frequencies. Images of *cloche* mutants (B,F) (with *sox7* and *sox18* probes, respectively) and siblings (A,E) (with *sox7* and *sox18* probes, respectively) are shown in dorsal views, anterior to the left; the expression of both genes in the PLM is lost in the mutants. The expression of *sox7* and *sox18* in nonvascular domains is unaffected in *cloche* mutants at 24 hpf, while most endothelial expression is lost (D,H) (*clo* embryos with *sox7* and *sox18* probes, respectively); (C,G) (siblings); lateral views, anterior to the left. The expression of *sox7* and *sox18* was analyzed by ISH in control embryos injected with std-MO and in *scl*-morphants at 6 to 8 somites (I,J,M,N) and 22 hpf (K,L,O,P). Control hybridizations on *scl*-morphants were carried out with *gata1* at both developmental stages. Comparable levels of *sox7* and *sox18* expression in the PLM are shown in control embryos (I,M) (with *sox7* and *sox18* probes, respectively) and in *scl*-morphants (J,N) (with *sox7* and *sox18* probes, respectively); dorsal views, anterior to the left. Expression of *sox18* (20 of 23) but not *sox7* (19 of 23) is detectable in the PCV region in *scl*-morphants at 22 hpf (L,P) (with *sox7* and *sox18* probes, respectively); std-MO–injected embryos are shown as a control (K,O) (with *sox7* and *sox18* probes, respectively); lateral views, anterior to the left. White arrowhead indicates DA; black arrowhead, PCV; black arrow, caudal vein (CV) region; and white asterisk, ICM.

and is required for hematopoietic and endothelial development.[26,52] At 6 to 8 somites, the expression of *sox7* and *sox18* in the ALM and PLM was lost in approximately one-quarter of the embryos (ie, in the expected *clo* homozygous mutants), along with a strong reduction in *gata1* signal (Figure 2A,B,E,F; data not shown). At 24 hpf, expression of *sox7* and *sox18* was detected in putative *clo* embryos only in nonvascular domains (Figure 2D,H). When embryos of the same clutch were hybridized with *cdh5* (coding for the endothelial-specific adhesion protein VE-cadherin), no expression was detectable in approximately one-quarter of the embryos except for a few cells in the cardinal vein plexus region, where also some residual *sox18* staining was noticeable (Figure 2H; data not shown). A few remaining endothelial cells have

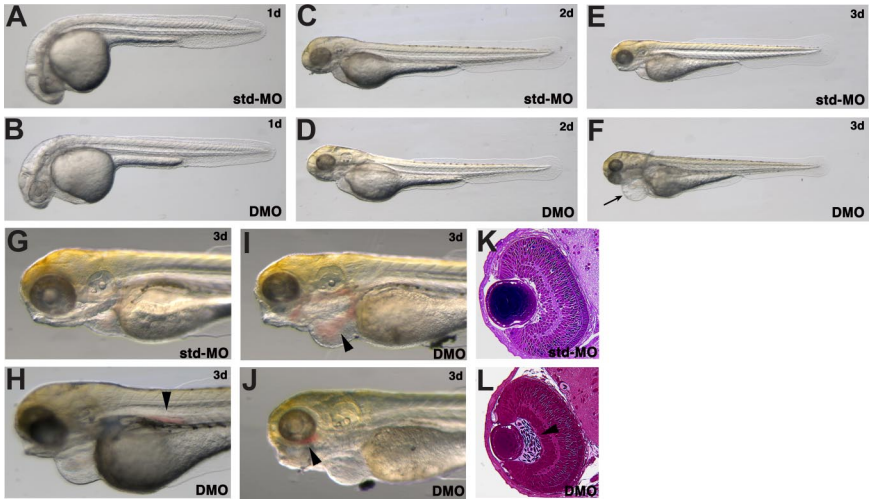


**Figure 3. The double knockdown of *sox7* and *sox18* does not cause gross morphologic abnormalities but selectively affects trunk/tail blood circulation.** Control embryos (A,C,E) were injected with a dose of std-MO (0.5 pmol) corresponding to the total dose of MOs injected in the double morphants. Low doses of *sox7*-MO1 and *sox18*-MO1 (0.25 pmol) were not causing gross morphologic defects when injected separately (Figure S3) or coinjected (DMO) (B,D,F). More than 90% of the double morphants showed no sign of trunk/tail blood circulation, while minor circulatory defects were detectable in single morphants (Table S1). (A,B) Control embryo and double morphant at 1 dpf. Images were taken at 32× magnification, anterior to the left. (C,D) control embryo and double morphant at 2 dpf. Images were taken at 25× magnification, anterior to the left. (E,F) control larva and double morphant at 3 dpf. Images were taken at 20× magnification, anterior to the left. By this stage, heart edema is clearly detectable in the double morphants (black arrow). (G-J) Images at 50× magnification of a control larva injected with std-MO (G), and 3 double morphants showing blood accumulation (black arrowheads) in the anterior trunk (H), in the heart to yolk region (I) where residual circulation is detectable, and in the eye region (J). Anterior to the left. (K,L) 132× magnification images of cross-sections at the level of the eye showing a control std-MO–injected embryo and a double morphant at 2 dpf. The black arrowhead points to blood accumulation in the inner optic circle in the double morphant. Anterior to the top.

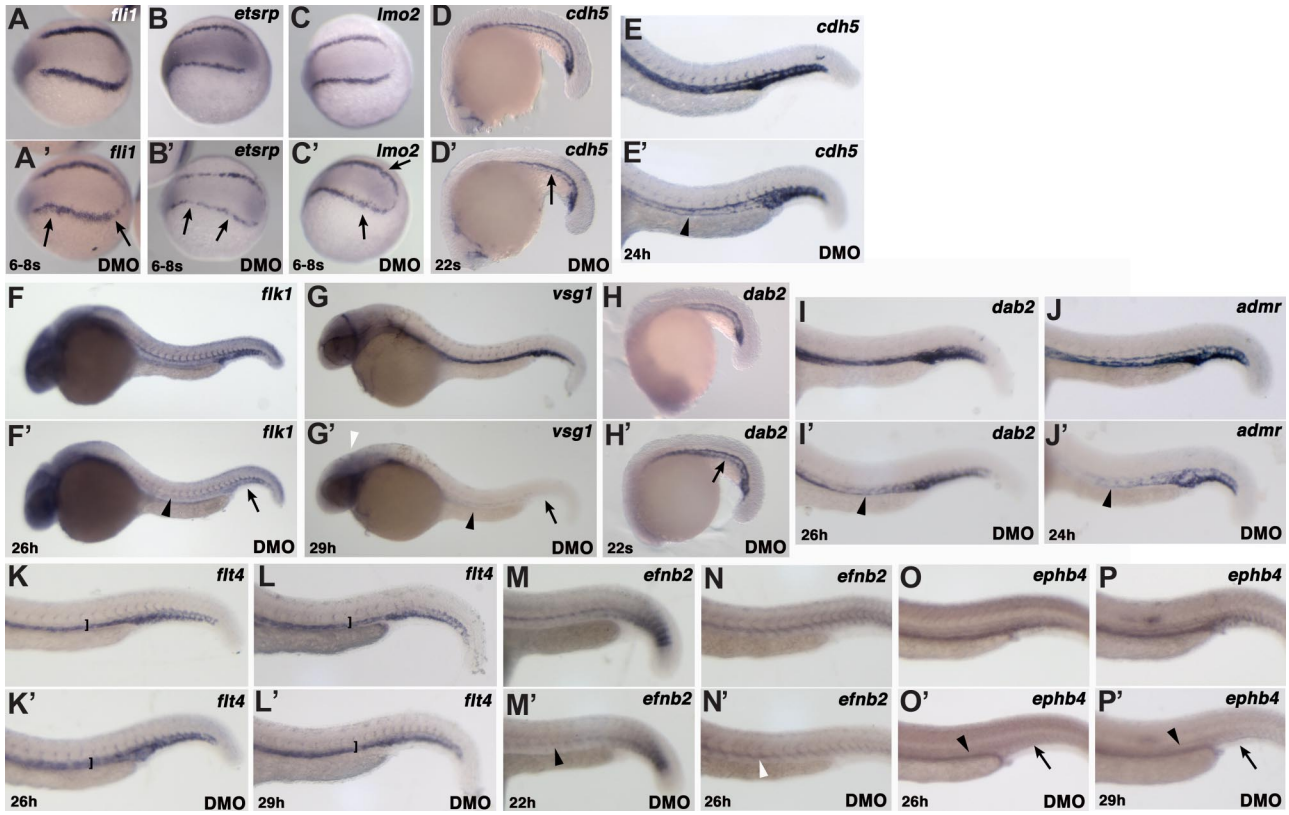


**Figure 4. The double knockdown of *sox18* and *sox7* differentially affects the expression of several endothelial markers.** We analyzed by ISH endothelial markers in control embryos and double morphants from 6 to 8 somites to 22 to 29 hpf. (A-P) Control embryos, ie, std-MO-injected embryos in all panels but panels C and J showing uninjected embryos. (A′-P′) Double morphants. Dorsal (A-C) or lateral views (D-P) are shown, anterior to the left, of whole embryos (40×) or trunk/tail regions (63×). (A-C) Dorsal views, showing expression of the indicated markers in the PLM. (A,A′) control uninjected and DMO embryos, respectively, at 6- to 8-somite stage probed with *fli1*. (B,B′) control std-MO and DMO embryos, respectively, at 6- to 8-somite stage probed with *etsrp*. The expression of *fli1* (8 of 11) and *etsrp* (8 of 11) appears slightly reduced and less organized in the double morphants. Black arrows point to particularly altered expression. (C,C′) control std-MO and DMO embryos, respectively, at 6- to 8-somite stage probed with *lmo2*. The expression of *lmo2* appears less organized (black arrows) in the DMOs (10 of 14). (D,D′) 22 somites, *cdh5*, panendothelial marker. The expression in the PCV (black arrow) is slightly reduced in the DMO embryos (15 of 18). (E,E′) 24 hpf, *cdh5*. The hybridization signal in the trunk/tail region is reduced mainly in the PCV (19 of 26; arrowhead). (F,F′) 26 hpf, *flk1*, preferentially expressed in arterial endothelial cells at this stage in control embryos. The hybridization signal is reduced in the axial vessels of the double morphants (10 of 17; black arrowhead pointing to DA, PCV; black arrow to CV region). (G,G′) 29 hpf, *vsg1*, mainly expressed in venous endothelial cells at this stage in control embryos. The expression is dramatically reduced in the double morphants (11 of 12; MCeV region, white arrowhead; PCV, black arrowhead; CV, arrow). (H,H′,I,I′) *dab2*, panendothelial marker at 22 somites, but mainly expressed in venous endothelial cells at 26 hpf in control embryos. The expression of *dab2* in the double morphants is not reduced in the PCV (black arrow) at 22 somites (13 of 18) but is reduced at 26 hpf (12 of 16; arrowhead). (J,J′) 24 hpf, *admr*, panendothelial marker with stronger expression in the PCV than in the DA in control embryos. The expression of *admr* (8 of 13) is reduced in the double morphants (arrowhead). (K,K′) 26hpf, *flt4*, venous endothelial marker at this stage in control embryos. The hybridization signal in axial vasculature is broader in the double morphants (11 of 18) than in control embryos (square bracket), possibly indicating an anomalous persistence of *flt4* expression in the DA. (L,L′) 29 hpf, *flt4*. The expression is now restricted to the PCV also in the double morphants (10 of 12). (M,M′, N,N′) 22 hpf and 26 hpf, respectively; *efnb2*, marking the DA. The signal in the DA is severely reduced at 22 hpf in the double morphants (13 of 19; black arrowhead), but becomes visible at 26 hpf (13 of 18; white arrowhead). (O,O′,P,P′) 26 hpf and 29 hpf, respectively; *ephb4*, marking the PCV and the underlying gut region. The signal in the PCV (arrowhead) and in the CV region (arrow) is severely reduced or absent in the double morphants (15 of 18 at 26 hpf, 8 of 11 at 29 hpf); staining in the gut region is still detectable. MCeV indicates middle cerebral vein.

indeed been observed in this region in *clo* mutants.[30,36,53] The vascular expression of *sox7* and *sox18* is thus controlled by *cloche*.

In contrast, the onset of *sox7* and *sox18* expression did not appear to be controlled by *scl*. In *scl*$^{mo}$ embryos, the expression pattern of *sox7* and *sox18* at 6 to 8 somites in the ALM and PLM was not altered (Figure 2; compare panels J,N with I,M), whereas *gata1* expression was absent or severely reduced (13 of 19; data not shown). The situation is different at 22 hpf: in *scl* morphants, the expression of *sox7* is limited to the developing otic vesicles, the region of the first aortic arch, and the ICM (Figure 2L), but *sox18*, similarly to *cdh5* (data not shown), is still expressed in the region of the posterior cardinal vein (PCV) and the caudal vein plexus (Figure 2P). As expected, *sox18* staining in the dorsal aorta (DA) and in the ISVs is absent, because of the crucial role of *scl* in the development of the DA.[26] Scl thus appears to control the maintenance of the endothelial expression of *sox7* but not of *sox18*.

Overall, the expression pattern of *sox7* and *sox18* genes points to a potential role in zebrafish vascular development.

### Double knockdown of *sox7* and *sox18* affects blood circulation

To test the hypothesis that *sox18* and *sox7* play redundant roles in vascular development, as suggested for mammalian homologs, we designed morpholinos against regions surrounding the AUG translation start codon of *sox18* or *sox7* (*sox18*-MO1 and *sox7*-MO1).

Low doses of morpholinos (250 fmol/embryo) caused no morphologic alterations when injected separately (Figure S3). When low doses of *sox18*-MO1 and *sox7*-MO1 were coinjected in the same embryos, gross morphologic abnormalities were absent at 1 dpf (Figure 3). However, functional defects started to appear after the onset of blood circulation and became more evident by 2 dpf (Table S1). More than 90% of the double morphants showed no sign of blood circulation in the trunk and

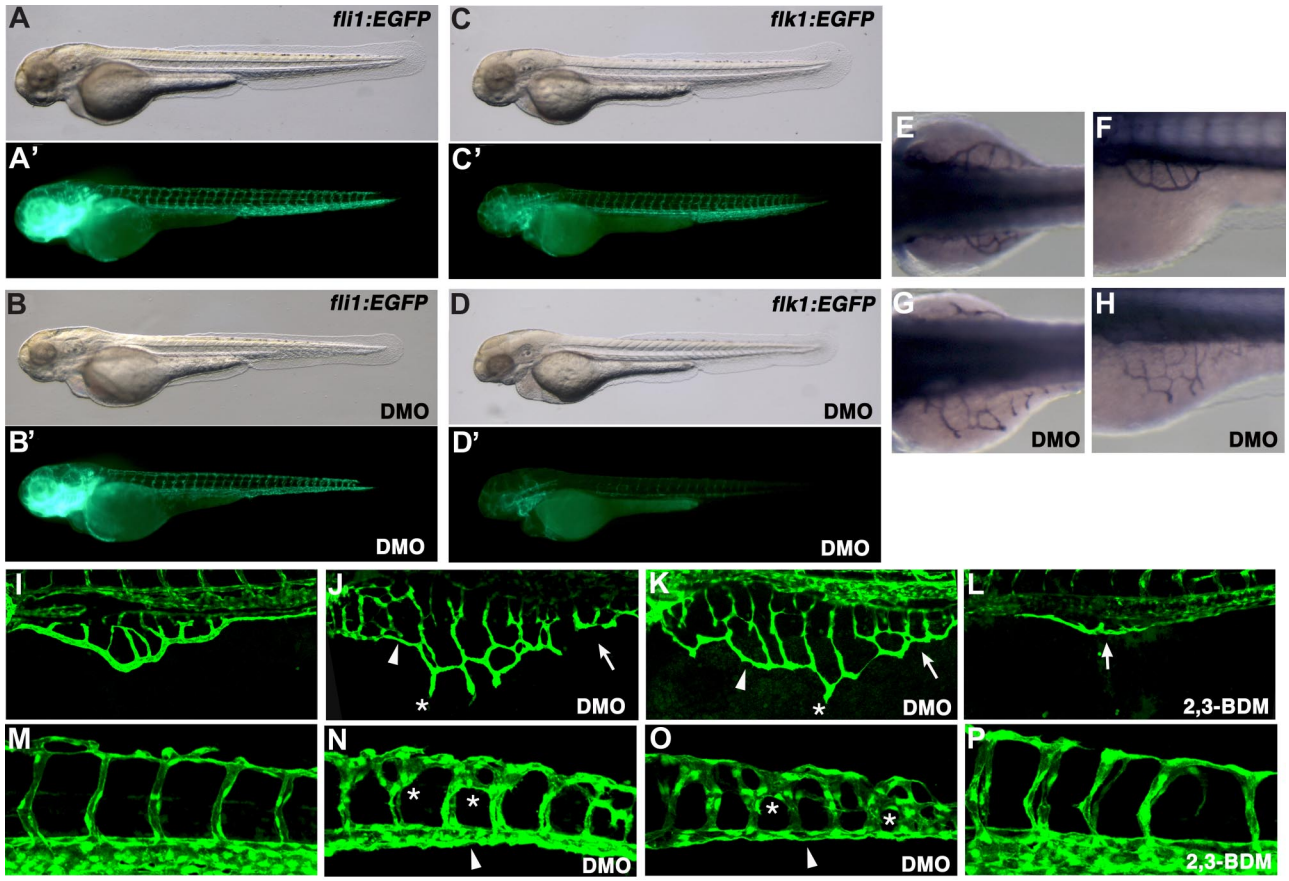


**Figure 5. The double knockdown of *sox18* and *sox7* affects vascular development.** We carefully analyzed the development of the vascular tree in the double morphants, using 2 different vascular-specific transgenic lines (ie, tg(*fli1*:EGFP)$^{y1}$ and tg(*flk1*:EGFP)). (A,A′-D,D′) lateral views, anterior to the left, of 2.5-dpf embryos; for each embryo, both brightfield (A-D) and fluorescence (A′-D′) stereomicroscopic images are shown. (A,A′,B,B′) control std-MO– and DMO-injected embryos, respectively, of the tg(*fli1*:EGFP)$^{y1}$ line. (C,C′-D,D′) control std-MO– and DMO-injected embryos, respectively, of the tg(*flk1*:EGFP) line. The expression of the transgene is not substantially reduced in the *fli1*:EGFP line, while it is dramatically reduced in the *flk1*:EGFP line upon double knockdown of *sox18* and *sox7*. (E-H) Staining of the endogenous AP activity was performed to analyze angiogenesis in the region of the subintestinal vessels (SIV) basket at 3 dpf. (E,F) control std-MO–injected embryos in dorsal and lateral views, respectively, anterior to the left. (G,H) DMO-injected embryos in dorsal and lateral views, respectively, anterior to the left. The SIV basket is severely disorganized and enlarged in the double morphants, showing thinner vessels and anomalous spikes pointing toward the yolk. (I,P) Confocal images of *fli1*:EGFP double morphants and control embryos showing the SIV basket (I-L) and the caudal intersomitic vessels (ISVs) (M-P) at 3 dpf. All lateral views, anterior to the left. (I,M) Control std-MO–injected embryos. (J,N) Embryos coinjected with *sox7*-MO1 and *sox18*-MO1, 125 fmol each. (K,O) Embryos coinjected with *sox7*-MO1 and *sox18*-MO1, 250 fmol each. (L,P) Control embryos treated with 2,3-BDM to block heartbeat and blood circulation. The alterations in the SIV basket and in the caudal ISVs visible in the double morphants are clearly distinct from the mere effect of absent blood flow. (J,K) Consistent with AP staining, confocal analysis reveals in the double morphants a global disorganization of the SIV basket, which is highly enlarged, particularly in the posterior aspect (white arrow). The caliber of most vessels in the basket, and especially of the subintestinal vein, is reduced in the double morphants (white arrowhead), which also present abnormal spikes toward the yolk (white asterisks). (L) The SIV basket appears instead reduced (white arrow) in the embryos treated with 2,3-BDM. (N,O) The caudal vein plexus (white arrowhead) is severely reduced in the double morphants, but not in 2,3-BDM–treated controls (P). In the double morphants (N,O), anomalous branching (white asterisks) is visible in the dorsal aspect of the caudal ISVs, pointing to defective proliferation/guidance mechanisms in angiogenic development. No abnormal branching of the ISVs is caused by a mere block in blood flow (P).

tail regions; blood flow was present only in the rostral part of the embryos, from heart to yolk through the anterior cardinal vein, on both sides or just on one side (Videos S1,S2). A premature venous return around the anus was observed in a few double morphants with residual limited blood flow in the trunk, possibly indicative of an AV shunt (Videos S3,S4).

By 3 dpf, a large number of double morphants showed extensive heart edema (Figure 3F), which we interpret as a secondary effect due to the block in circulation. Many double morphants showed blood poolings in various positions, including eyes, trunk, and pericardiac region (Figure 3H-J,L).

Another set of morpholinos (*sox18*-MO4 and *sox7*-MO4), targeting different sequences in the 5′ UTR of *sox18* or *sox7* transcripts, gave qualitatively similar results (Table S1). This confirms that the massive circulatory phenotype is specifically linked to knockdown of both genes, but not of either gene at a time. When combined, the 2 sets of morpholinos could cause a massive circulatory phenotype even at doses that were basically ineffective on their own, confirming their targeting specificity (Table S1). Splice morpholinos (*sox18*-MO2 and *sox7*-MO2) interfering with the maturation of *sox18* and *sox7* transcripts also reproduced the circulatory phenotype when combined, though with a lower penetrance (Figure S4; Table S2).

### Double knockdown of *sox7* and *sox18* affects the expression of endogenous endothelial markers

To gain insight into the molecular events following the double knockdown of *sox7* and *sox18*, we analyzed the expression of several endothelial and nonendothelial markers. A subtle reduction and/or partial disorganization in the expression of *fli1*, *etsrp*, and *lmo2* genes in the PLM was detectable by ISH in the double morphants at early somitogenesis (Figure 4A,A′-C,C′), whereas the expression of *scl* and of the early hematopoietic markers *gata2* and *gata1* appeared unaffected (Figure S5; data not shown).

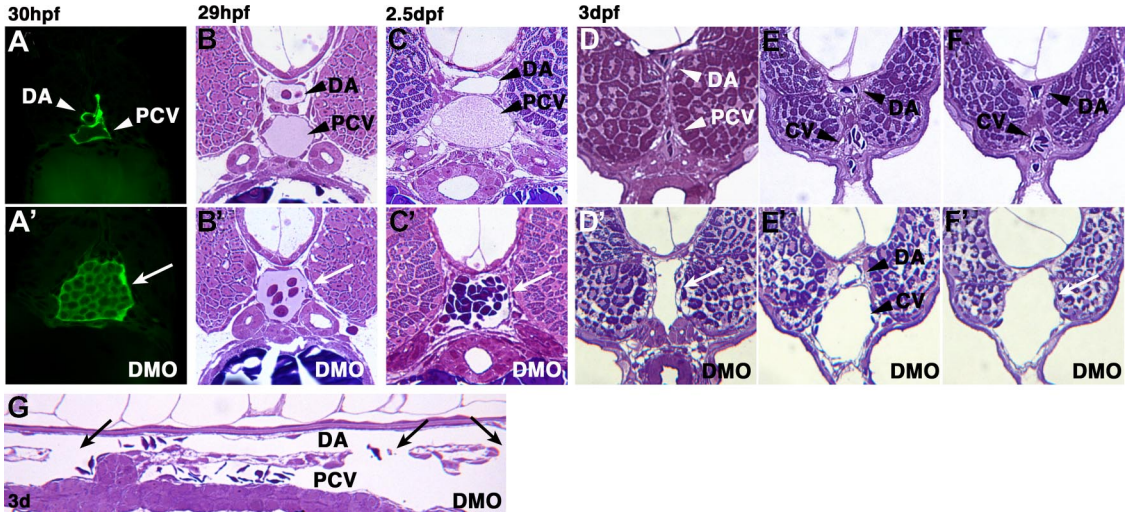


**Figure 6. The double knockdown of *sox18* and *sox7* results in multiple AV shunts.** We analyzed sections from control embryos and double morphants from 29-30 hpf to 3 dpf, using both the *fli1*:EGFP line and a wild-type background. Multiple AV shunts between the DA and the axial vein are visible in the trunk/tail region of the double morphants. (A,A′) fluorescent images of cross sections of a control std-MO–injected embryo (A) and a double morphant (A′) at 30 hpf, in the tg(*fli1*:EGFP)$^{y1}$ line. Two distinct vessels, corresponding to the DA and the PCV (arrowheads), surrounded by fluorescent endothelial cells, are visible in the control, whereas a single, enlarged vessel full of presumptive blood cells is present in the double morphant's section (arrow). (B,B′) Cross sections of a control std-MO–injected embryo (B) and a double morphant (B′) at 29 hpf, showing an AV fusion. (C,C′) cross sections of a control std-MO–injected embryo (C) and a double morphant (C′) at 2.5 dpf, showing an AV fusion with putative blood clot. (D,D′-F,F′) a rostro-caudal series of cross sections, before (D,D′) or after the anus (E,E′,F,F′) showing control std-MO–injected embryos (D-F) and a double morphant (D′-F′) at 3 dpf. The axial artery and vein are fused in panels D′ and F′, but not in E′ (ie, multiple fusions occur along the axial vessels, as documented also in panel G). (G) longitudinal section of a 3-dpf double morphant, anterior to the left. A separation is visible, in the central part of the panel, between the DA and the PCV (the notochord is clearly visible above the DA, and the gut below the PCV), but multiple AV shunts are detectable (arrows), allowing blood cells to freely move from one vessel to the other.

A reduced expression of *cdh5*, but not of other endothelial markers, in the primordium of the PCV was noticed at 22 somites (Figure 4D,D′, H,H′; data not shown).

At 22 to 26 hpf, around the normal onset of blood circulation in control embryos, the expression of several endothelial markers (*flk1,* the vessel-specific gene 1 [*vsg1*], *cdh5*, the adrenomedullin receptor [*admr*], and *dab2*) appeared reduced in the double morphants, particularly in the trunk/tail region (Figure 4E,E′-G,G′,I,I′,J,J′). These defects were particularly evident in the PCV and in the caudal vein plexus.

Endothelial expression of some markers was specifically delayed in the double morphants. Arterial expression of *flt4*, for example, persisted in the double morphants at 26 hpf, whereas it was already restricted to venous endothelial cells in control embryos (Figure 4K,K′). The vein-specific expression of *flt4* was indeed only detectable at 29 hpf in the double morphants (Figure 4L,L′). The expression of ephrinB2 (*efnb2a*) in the DA was markedly reduced in the double morphants at 22 hpf (Figure 4M,M′), but became comparable with control embryos by 26 hpf (Figure 4N,N′). Very little or no expression of the venous marker *ephb4* could be detected in the caudal vein plexus region of the double morphants in the same interval and even at a later stage (29 hpf; Figure 4O,O′,P,P′).

In contrast, double knockdown of *sox7* and *sox18* does not alter the expression of DA markers such as *gridlock* (*grl*), *notch3*, *deltaC*, and *kdrb* genes (Figure S5; data not shown). A number of genes (*vegf*, angiopoietin 1 [*ang1*], the growth differentiation factor 6a [*gdf6a*]/*radar*) expressed in nonendothelial cells are known to influence vascular development, but their expression was not affected in the double morphants (Figure S5; data not shown).

The ISH analysis of key markers on double morphants injected with the second set of morpholinos (DMO4) gave qualitatively similar, though quantitatively less pronounced, results (Figure S6). The same markers were unaffected in the single morphants.

These data support the notion that *sox7* and *sox18* have a role in the establishment of the venous identity.

### Double knockdown of *sox7* and *sox18* affects the expression of reporter genes in vascular specific transgenic lines

To better characterize vascular abnormalities, we made use of the tg(*fli1*:EGFP)$^{y1}$ transgenic line,[22] where the enhanced green fluorescent protein (EGFP) expression is driven by the promoter region of the early endothelial gene *fli1*. The overall fluorescence of this transgenic line is not substantially affected by the double knockdown of *sox7* and *sox18* (compare Figure 5A′ with 5B′), thus enabling us to use confocal microscopy to better define vascular defects. Starting from 2 dpf, the subintestinal vessels (SIVs) basket showed severe abnormalities in the double morphants, as also revealed by endogenous alkaline phosphatase (AP) staining at 3 dpf (Figure 5J,K and G,H). The SIV basket appeared less regularly organized and severely enlarged, with thinner vessels and very elongated spikes protruding toward the yolk. No enlargement of the SIV basket was associated with 2,3-BDM treatment, which weakens myocardial force through a block of myofibrillar ATPase and therefore eliminates blood flow[43] (Figure 5L).

Vascular defects were also detectable in the caudal region. The caudal vein plexus was severely reduced. Moreover, the double morphants showed enlarged, not patent ISVs with increased vessel branching and aberrant anastomoses, particularly in the dorsal somites (Figure 5N,O). The simple block of blood flow induced with 2,3-BDM did not induce similar abnormalities, apart from some thickening of the caudal ISVs (Figure 5P).

Coinjection of *sox18*-MO1 and *sox7*-MO1 in the tg(*flk1*:EGFP) line led to a severe reduction in the expression of the transgene which is driven by the *flk1/vegfr2/kdra* promoter. Residual fluorescence in the trunk axial vessels is limited to the DA (Figure 5D′). The strong difference in EGFP fluorescence in the 2 transgenic lines, together with the fact that *fli1* is expressed earlier than *flk1* in

endothelial development, lead us to conclude that endothelial cells are specified but do not properly follow their differentiation program when *sox7* and *sox18* are simultaneously knocked down.

### Double knockdown of *sox7* and *sox18* causes fusions of the axial vessels

The ISH analysis suggested that the alterations in the expression of endothelial markers in the double morphants were more pronounced in the trunk/tail region and more profound in the axial vein than in the DA.

Histologic analysis was carried out on double morphants starting from 29 hpf. In the anterior trunk (ie, in the region of DA/PCV bifurcations), a single axial vessel was detectable in 1 or 2 points due to shunts between the DA and the PCV (Figure 6B′). The fusion of the DA and PCV endothelia in the trunk was also clearly visible in cryosections of tg(*fli1*:EGFP)$^{y1}$ double morphant embryos at 30 hpf (Figure 6A′). Around this stage, arteriovenous shunts leading to premature blood flow return in the arterior trunk were also visible in vivo in double morphants (Videos S5,S6). The anterior trunk fusions were clearly detectable also at 2.5 dpf and 3 dpf (Figure 6C′; data not shown).

By 3 dpf, the axial vein was significantly dilated in the trunk/tail region whereas the separation between the major axial vessels was reduced (Figure 6E′). These anomalies were also present in control embryos treated with 2,3-BDM (Figure S7) and could therefore be due to the lack of blood flow. In the double morphants, multiple AV shunts between the axial vessels were detectable in the posterior trunk/tail region starting from 2.5 dpf and became more extended with development (Figure 6D′,F′,G). On the contrary, no AV fusions were present in 2,3-BDM–treated embryos (Figure S7).

We conclude that the extensive AV shunts in the tail of the double morphants are late events specifically due to the *sox7*/*sox18* double knockdown, whereas axial vascular tube formation per se is not affected. Our histologic analysis reveals putative occluding thrombi followed by huge blood poolings at or just following some of the AV shunts in the trunk (data not shown; Figure 6A′,C′).

## Discussion

We used zebrafish as a model system to study the role of Sox18 in endothelial cell differentiation and vascular development and to directly test the hypothesis of functional redundancy among Sox-F proteins.

We identified single-copy genes as bona fide *sox18* and *sox7*. Our real-time RT-PCR analysis revealed that *sox18* and *sox7* have similar temporal expression patterns and suggested that they both act from early somitogenesis. In contrast, *sox17* is mainly expressed during gastrulation and its expression drops afterward. The residual *sox17* expression reported in somitogenesis with a transgenic line is limited to endodermal cells.[54] In contrast, all 3 Sox-F members are coexpressed in vascular endothelial cells, and *Sox17* and *Sox18* act redundantly in postnatal angiogenesis in mice.[55]

Both *sox18* and *sox7* are expressed at very early steps of endothelial differentiation as: in the anterior and posterior lateral plate mesoderm, where endothelial cell precursors reside; in the angioblasts migrating toward the midline and coalescing to form the main axial artery and vein; in the endothelial cells of the nascent intersomitic vessels; and in the forming head vasculature. Each gene also shows unique expression domains (eg, in the central nervous system or in the otic vesicles), suggesting that they act redundantly in vascular development while acting nonredundantly in other developmental processes.

Endothelial expression of *sox18* and *sox7* is differently regulated: *scl* controls the endothelial expression of *sox7*, but not of *sox18*, at 22 hpf. *scl* knockdown does not affect their initial expression, consistent with the model in which *scl* acts downstream of *cloche*, playing a role in vascular development but not in the very initial phases of endothelial cell development, where instead *etsrp* would be a major player.[56,57]

Knocking down each single gene caused no or limited effect on blood circulation. In contrast, the double knockdown of *sox18* and *sox7* led to a massive and specific block in trunk/tail blood circulation. The effects of the combined knockdown of the 2 genes are more than additive, strongly implying that *sox18* and *sox7* act redundantly in vascular development. In contrast, our preliminary knockdown experiments with morpholinos against *sox18* and *sox17* did not reveal functional redundancy in zebrafish vascular development. It is noteworthy that SOX7 and SOX18 proteins were shown to be functionally redundant in cardiogenesis in *Xenopus*.[58]

The emerging picture is that the double knockdown of *sox18* and *sox7* disturbs the normal acquisition of specific markers during endothelial cell differentiation. More specifically, the acquisition of the correct AV identity appears to be impaired. In axial veins, we found a moderate to strong reduction in the expression of panendothelial or venous markers. The expression of both ephrinB2 and EphB4 was affected, though differently since venous expression of EphB4 was stably reduced, while arterial expression of ephrinB2 appeared only transiently affected. In contrast, at the developmental stages we analyzed we could not detect alterations in several genes controlling arterial differentiation.

A common outcome of the lack of proper AV identity is the formation of AV shunts. Mutations or functional knockdown of genes of the Notch pathway, controlling arterial differentiation, and endothelial-specific overexpression of COUP-TFII, which controls vein identity, all lead to fusion of arteries and veins.[1,5,59,60] A similar picture emerges in *sox18*/*sox7* double morphants in which we describe the presence of AV shunts at developmental stages close to the first onset of blood circulation.

Already at 29 hpf, AV shunts can be clearly detected in the trunk region of the double morphants, the DA being fused to the PCV. The fusions occur in recurrent sites along the axial vessels, and histologic analysis reveals that the extent of the AV shunts increases as development proceeds. At 3 dpf, multiple AV shunts lead to a single dilated axial vessel in the double morphants' tails, though distinct DA and CV (caudal vein) initially form. In the vast majority of the double morphants, no blood flow is detectable in the trunk/tail region, although the formation of the AV shunts is not apparently linked to the consequent change in hemodynamic forces. In fact, a chemical treatment blocking blood flow (2,3-BDM) does not result in AV fusions, and no such AVM have been reported for *silent heart/tnnt2* (*sih*) MO-injected embryos, which also lack circulation.[61]

Anomalous fusions of arterioles and venules can lead to telangiectases, as reported in patients with HHT.[7] It is tempting to speculate that our studies in zebrafish are unraveling a molecular basis for telangiectases in patients with HLT carrying mutations in *SOX18*.[9]

Endothelial cells from blood vessels of different caliber or anatomical sites are distinct differentiated cell types with distinct intrinsic gene expression programs,[62] exposed to different extrinsic influences.[6] Consistently, in the *sox18/sox7* double morphants, the alteration in the expression of the affected genes is, in general,

more pronounced in the trunk/tail region than in the head. Axial vessels, and in particular the PCV and the caudal vein plexus, appear more affected than the ISVs in our ISH analyses. Nevertheless, the most caudal ISVs are specifically altered in the double morphants, as they appear thickened, not lumenized, and show anomalous branching in their dorsalmost aspect. The SIV basket, which is highly enlarged in the double morphants, presents instead thinner vessels than in control larvae. These vessels are more irregularly shaped and present abnormal spikes protruding toward the yolk. Overall, these observations suggest that the role of *sox18* and *sox7* is specific for different regions of the vascular tree.

In conclusion, we introduce here novel concepts on the role of *sox18* and *sox7* in endothelial cell differentiation and vascular development. We report that these genes act in concert at very early stages of angioblast differentiation and, most important, control the acquisition of AV identity. The described vascular phenotype, characterized by AV shunts, suggests links to the human HLT syndrome associated with mutations in the *SOX18* gene. This supports the use of zebrafish to help deciphering the molecular basis of hereditary vascular diseases.

Lymphedema is the most prominent feature of the human HLT syndrome. It is worth noting that lymphatic endothelial cells derive from venous endothelial cells both in mammals[63] and, as recently reported, in zebrafish.[64,65] The double knockdown of zebrafish *sox7* and *sox18* affects mainly venous endothelial cell differentiation; it will be therefore interesting to address whether they also have a role in lymphatic endothelial cell differentiation.

## Acknowledgments

We would like to thank the following colleagues for probes and reagents: M. Gering, R. Patient, N. Lawson, S. Schulte-Merker, B. Weinstein, S. Sumanas, J. Larson, D. Stainier, C. Wilson, S. Wilson, Z. Wen, K. Crosier, and F. Argenton. We appreciate the help of A. Conti and F. Orsenigo for the analysis of quantitative PCR results, and of S. Rodighiero for confocal analysis. We would like to thank C. Lora-Lamia for teaching us histologic techniques, G. Cappellano for his contribution to the initial phase of this project, G. Brunetti for his help in fish husbandry, S. Nicoli and A. Rissone for helpful suggestions, and M. E. Bianchi and M. Presta for critical reading of the manuscript.

We acknowledge financial support from the Telethon Foundation (GGP04255 to M.B.), Italian Ministry of Education, University, and Research (MIUR-Cofin 2004 to M.B. and Cofin 2006 to E.D.), Fondazione Cariplo (Cariplo 2006 to M.B. and N.O.B.E.L. to F.C.), Leducq Foundation, and Istituto Superiore di Sanità (project on Rare diseases to E.D.). S.M. is the recipient of a PhD fellowship from the Fondazione Fratelli Confalonieri.

## Authorship

Contribution: S. Cermenati and S.M. performed research and analyzed data; S. Cimbro, P.C., L.D.G., and R.A. participated in performing research; P.K. discussed the results and provided helpful suggestions; E.D. and F.C. analyzed data and provided helpful suggestions; and M.B. designed and supervised the research project, analyzed data, and wrote the paper.

Conflict-of-interest disclosure: The authors declare no competing financial interests.

Correspondence: Monica Beltrame, Dipartimento di Scienze Biomolecolari e Biotecnologie, Università degli Studi di Milano, Via Celoria 26, 20133 Milano, Italy; e-mail: monica.beltrame@unimi.it.

## References

1. Lawson ND, Scheer N, Pham VN, et al. Notch signaling is required for arterial-venous differentiation during embryonic vascular development. Development. 2001;128:3675-3683.
2. Zhong TP, Childs S, Leu JP, Fishman MC. Gridlock signalling pathway fashions the first embryonic artery. Nature. 2001;414:216-220.
3. Lawson ND, Vogel AM, Weinstein BM. sonic hedgehog and vascular endothelial growth factor act upstream of the Notch pathway during arterial endothelial differentiation. Dev Cell. 2002;3:127-136.
4. Rossant J, Hirashima M. Vascular development and patterning: making the right choices. Curr Opin Genet Dev. 2003;13:408-412.
5. You LR, Lin FJ, Lee CT, DeMayo FJ, Tsai MJ, Tsai SY. Suppression of Notch signalling by the COUP-TFII transcription factor regulates vein identity. Nature. 2005;435:98-104.
6. Coultas L, Chawengsaksophak K, Rossant J. Endothelial cells and VEGF in vascular development. Nature. 2005;438:937-945.
7. Hirashima M, Suda T. Differentiation of arterial and venous endothelial cells and vascular morphogenesis. Endothelium. 2006;13:137-145.
8. Urness LD, Sorensen LK, Li DY. Arteriovenous malformations in mice lacking activin receptor-like kinase-1. Nat Genet. 2000;26:328-331.
9. Irrthum A, Devriendt K, Chitayat D, et al. Mutations in the transcription factor gene SOX18 underlie recessive and dominant forms of hypotrichosis-lymphedema-telangiectasia. Am J Hum Genet. 2003;72:1470-1478.
10. Wegner M. From head to toes: the multiple facets of Sox proteins. Nucleic Acids Res. 1999;27:1409-1420.
11. Bowles J, Schepers G, Koopman P. Phylogeny of the SOX family of developmental transcription factors based on sequence and structural indicators. Dev Biol. 2000;227:239-255.
12. Schepers GE, Teasdale RD, Koopman P. Twenty pairs of Sox: extent, homology, and nomenclature of the mouse and human Sox transcription factor gene families. Dev Cell. 2002;3:167-170.
13. Carter TC, Phillips RJS. Ragged, a semidominant coat texture mutant in the house mouse. J Hered. 1954;45:151-154.
14. Slee J. The morphology and development of ragged—a mutant affecting the skin and hair of the house mouse: II, Genetics, embriology and gross juvenile morphology. J Genet. 1957;55:570-584.
15. Pennisi D, Gardner J, Chambers D, et al. Mutations in Sox18 underlie cardiovascular and hair follicle defects in ragged mice. Nat Genet. 2000; 24:434-437.
16. James K, Hosking B, Gardner J, Muscat GE, Koopman P. Sox18 mutations in the ragged mouse alleles ragged-like and opossum. Genesis. 2003;36:1-6.
17. Green E, Mann S. Opossum, a semi-dominant lethal mutation affecting hair and other characteristics of mice. J Hered. 1961;52:223-227.
18. Pennisi D, Bowles J, Nagy A, Muscat G, Koopman P. Mice null for Sox18 are viable and display a mild coat defect. Mol Cell Biol. 2000;20:9331-9336.
19. Downes M, Koopman P. SOX18 and the transcriptional regulation of blood vessel development. Trends Cardiovasc Med. 2001;11:318-324.
20. Young N, Hahn CN, Poh A, et al. Effect of disrupted SOX18 transcription factor function on tumor growth, vascularization, and endothelial development. J Natl Cancer Inst. 2006;98:1060-1067.
21. Westerfield M. The Zebrafish Book. Eugene, OR: University of Oregon Press; 1993.
22. Lawson ND, Weinstein BM. In vivo imaging of embryonic vascular development using transgenic zebrafish. Dev Biol. 2002;248:307-318.
23. Jin SW, Beis D, Mitchell T, Chen JN, Stainier DY. Cellular and molecular analyses of vascular tube and lumen formation in zebrafish. Development. 2005;132:5199-5209.
24. Traver D, Paw BH, Poss KD, Penberthy WT, Lin S, Zon LI. Transplantation and in vivo imaging of multilineage engraftment in zebrafish bloodless mutants. Nat Immunol. 2003;4:1238-1246.
25. Nasevicius A, Ekker SC. Effective targeted gene "knockdown" in zebrafish. Nat Genet. 2000;26: 216-220.
26. Patterson LJ, Gering M, Patient R. Scl is required for dorsal aorta as well as blood formation in zebrafish embryos. Blood. 2005;105:3502-3511.
27. Argenton F, Giudici S, Deflorian G, Cimbro S, Cotelli F, Beltrame M. Ectopic expression and knockdown of a zebrafish sox21 reveal its role as a transcriptional repressor in early development. Mech Dev. 2004;121:131-142.
28. Fouquet B, Weinstein BM, Serluca FC, Fishman MC. Vessel patterning in the embryo of the zebrafish: guidance by notochord. Dev Biol. 1997; 183:37-48.

29. Brown LA, Rodaway AR, Schilling TF, et al. Insights into early vasculogenesis revealed by expression of the ETS-domain transcription factor Fli-1 in wild-type and mutant zebrafish embryos. Mech Dev. 2000;90:237-252.
30. Thompson MA, Ransom DG, Pratt SJ, et al. The cloche and spadetail genes differentially affect hematopoiesis and vasculogenesis. Dev Biol. 1998;197:248-269.
31. Detrich HW, 3rd Kieran MW, Chan FY, et al. Intraembryonic hematopoietic cell migration during vertebrate development. Proc Natl Acad Sci U S A. 1995;92:10713-10717.
32. Smithers L, Haddon C, Jiang YJ, Lewis J. Sequence and embryonic expression of deltaC in the zebrafish. Mech Dev. 2000;90:119-123.
33. Gering M, Rodaway AR, Gottgens B, Patient RK, Green AR. The SCL gene specifies haemangioblast development from early mesoderm. EMBO J. 1998;17:4029-4045.
34. Liang D, Xu X, Chin AJ, et al. Cloning and characterization of vascular endothelial growth factor (VEGF) from zebrafish, Danio rerio. Biochim Biophys Acta. 1998;1397:14-20.
35. Song HD, Sun XJ, Deng M, et al. Hematopoietic gene expression profile in zebrafish kidney marrow. Proc Natl Acad Sci U S A. 2004;101:16240-16245.
36. Sumanas S, Jorniak T, Lin S. Identification of novel vascular endothelial-specific genes by the microarray analysis of the zebrafish cloche mutants. Blood. 2005;106:534-541.
37. Pham VN, Roman BL, Weinstein BM. Isolation and expression analysis of three zebrafish angiopoietin genes. Dev Dyn. 2001;221:470-474.
38. Crosier PS, Kalev-Zylinska ML, Hall CJ, Flores MV, Horsfield JA, Crosier KE. Pathways in blood and vessel development revealed through zebrafish genetics. Int J Dev Biol. 2002;46:493-502.
39. Larson JD, Wadman SA, Chen E, et al. Expression of VE-cadherin in zebrafish embryos: a new tool to evaluate vascular development. Dev Dyn. 2004;231:204-213.
40. Qian F, Zhen F, Ong C, et al. Microarray analysis of zebrafish cloche mutant using amplified cDNA and identification of potential downstream target genes. Dev Dyn. 2005;233:1163-1172.
41. Covassin LD, Villefranc JA, Kacergis MC, Weinstein BM, Lawson ND. Distinct genetic interactions between multiple Vegf receptors are required for development of different blood vessel types in zebrafish. Proc Natl Acad Sci U S A. 2006;103:6554-6559.
42. Nicoli S, Ribatti D, Cotelli F, Presta M. Mammalian tumor xenografts induce neovascularization in zebrafish embryos. Cancer Res. 2007;67:2927-2931.
43. Bartman T, Walsh EC, Wen KK, et al. Early myocardial function affects endocardial cushion development in zebrafish. PLoS Biol. 2004;2:e129.
44. Sinner D, Rankin S, Lee M, Zorn AM. Sox17 and beta-catenin cooperate to regulate the transcription of endodermal genes. Development. 2004;131:3069-3080.
45. Postlethwait JH, Woods IG, Ngo-Hazelett P, et al. Zebrafish comparative genomics and the origins of vertebrate chromosomes. Genome Res. 2000;10:1890-1902.
46. Alexander J, Stainier DY. A molecular pathway leading to endoderm formation in zebrafish. Curr Biol. 1999;9:1147-1157.
47. Takash W, Canizares J, Bonneaud N, et al. SOX7 transcription factor: sequence, chromosomal localisation, expression, transactivation and interference with Wnt signalling. Nucleic Acids Res. 2001;29:4274-4283.
48. Fawcett SR, Klymkowsky MW. Embryonic expression of Xenopus laevis SOX7. Gene Expr Patterns. 2004;4:29-33.
49. Gering M, Yamada Y, Rabbitts TH, Patient RK. Lmo2 and Scl/Tal1 convert non-axial mesoderm into haemangioblasts which differentiate into endothelial cells in the absence of Gata1. Development. 2003;130:6187-6199.
50. Stainier DY, Weinstein BM, Detrich HW 3rd, Zon LI, Fishman MC. cloche, an early acting zebrafish gene, is required by both the endothelial and hematopoietic lineages. Development. 1995;121:3141-3150.
51. Liao EC, Paw BH, Oates AC, Pratt SJ, Postlethwait JH, Zon LI. SCL/Tal-1 transcription factor acts downstream of cloche to specify hematopoietic and vascular progenitors in zebrafish. Genes Dev. 1998;12:621-626.
52. Dooley KA, Davidson AJ, Zon LI. Zebrafish scl functions independently in hematopoietic and endothelial development. Dev Biol. 2005;277:522-536.
53. Liao W, Bisgrove BW, Sawyer H, et al. The zebrafish gene cloche acts upstream of a flk-1 homologue to regulate endothelial cell differentiation. Development. 1997;124:381-389.
54. Sakaguchi T, Kikuchi Y, Kuroiwa A, Takeda H, Stainier DY. The yolk syncytial layer regulates myocardial migration by influencing extracellular matrix assembly in zebrafish. Development. 2006;133:4063-4072.
55. Matsui T, Kanai-Azuma M, Hara K, et al. Redundant roles of Sox17 and Sox18 in postnatal angiogenesis in mice. J Cell Sci. 2006;119:3513-3526.
56. Patterson LJ, Patient R. The "Ets" factor: vessel formation in zebrafish—the missing link? PLoS Biol. 2006;4:e24.
57. Sumanas S, Lin S. Ets1-related protein is a key regulator of vasculogenesis in zebrafish. PLoS Biol. 2006;4:e10.
58. Zhang C, Basta T, Klymkowsky MW. SOX7 and SOX18 are essential for cardiogenesis in Xenopus. Dev Dyn. 2005;234:878-891.
59. Duarte A, Hirashima M, Benedito R, et al. Dosage-sensitive requirement for mouse Dll4 in artery development. Genes Dev. 2004;18:2474-2478.
60. Krebs LT, Shutter JR, Tanigaki K, Honjo T, Stark KL, Gridley T. Haploinsufficient lethality and formation of arteriovenous malformations in Notch pathway mutants. Genes Dev. 2004;18:2469-2473.
61. Jin SW, Herzog W, Santoro MM, et al. A transgene-assisted genetic screen identifies essential regulators of vascular development in vertebrate embryos. Dev Biol. 2007;307:29-42.
62. Chi JT, Chang HY, Haraldsen G, et al. Endothelial cell diversity revealed by global expression profiling. Proc Natl Acad Sci U S A. 2003;100:10623-10628.
63. Oliver G, Alitalo K. The lymphatic vasculature: recent progress and paradigms. Annu Rev Cell Dev Biol. 2005;21:457-483.
64. Yaniv K, Isogai S, Castranova D, Dye L, Hitomi J, Weinstein BM. Live imaging of lymphatic development in the zebrafish. Nat Med. 2006;12:711-716.
65. Kuchler AM, Gjini E, Peterson-Maduro J, Cancilla B, Wolburg H, Schulte-Merker S. Development of the zebrafish lymphatic system requires VEGFC signaling. Curr Biol. 2006;16:1244-1248.